Lidar and true-orthorectification of infrared aerial imagery of high *Pinus sylvestris* forest in mountainous relief

Rubén VALBUENA[1], Tomás FERNÁNDEZ DE SEVILLA[2], Francisco MAURO[1], Cristina PASCUAL[1], Antonio GARCÍA-ABRIL[1], Susana MARTÍN[1] & José Antonio MANZANERA[1]

[1] Technical University of Madrid (UPM). Research Group for Sustainable Management (Tecnatura). Forestry Faculty. Ciudad Universitaria s/n. 28040 Madrid. Spain.
r.valbuena@upm.es
[2] Stereocarto S.L. Paseo de la Habana 200. 28036 Madrid. Spain.
tfsevilla@stereocarto.com

Abstract

Combination of various data sources has been demonstrated more effective than using them separately. Information retrieval is significantly improved by synergies between laser scanner and optical imagery. Digital photography relies on traditional methods for orthorectification in order to accomplish an accurate correspondence with Lidar. We investigated combinatorial techniques in a high pine forest situated in mountainous relief in the Guadarrama Range (Spain). Results have shown critical inaccuracies in the integration of these data, even when obtained simultaneously. We propose the use of Lidar-derived Digital Surface Model in the process of orthorectification of aerial imagery. We hypothesised that the use of true-orthophoto techniques for improving the planimetric accuracy of VHR can be reliable for forestry applications. The methodology slightly improved the geometrical results obtained, though radiometric results might be meaningless. Consequently, other possible solutions are also discussed.

Keywords: LiDAR, color infrared, true-orthorrectification, forest management.

1. Introduction

Very High Resolution (VHR) optical imagery and Lidar have synergic capabilities for providing reliable data in operational forestry. For this reason, the integration of these data allows a cost-effective combination of techniques. Methodologies can benefit from the possibilities of both sensors: the potential of VHR imagery for thematic classification and index calculation (St-Onge and Cavayas 1997), and the accuracy of tree height information retrieved from Lidar (Lefsky *et al*. 1999). Extraction of Digital Elevation Models (DEM) from simultaneous Lidar can improve the automation of VHR imagery orthorectification. Information retrieval from Lidar can be also assisted by VHR. For instance, individual trees can be recognized and segmented from VHR imagery and their height and crown shape properties calculated from the Lidar point cloud (Leckie *et al.* 2005; Suárez *et al.* 2005).

Lidar can be used for improved traditional photogrametric methods. It has been demonstrated that tree height retrieved from Lidar is more reliable than photogrametry, since shade often obscures bare soil on aerial images (Hyyppä *et al*. 2008). Correlation of image pairs for mass point detection is time-consuming because it requires the quality control of a technician. Thus, correlation has been demonstrated inefficient in forest areas with high dense canopy, though other automated matching techniques are being developed (Zhang and Gruen 2004). For this reason, traditional photogrametry has been demonstrated insufficient for large scale forest monitoring (St-Onge and Achaichia 2001). Waser *et al.* (2008) used Lidar data for normalizing a DEM retrieved from correlation of Colour Infra Red (CIR) aerial images.

In order to integrate the information derived from diverse sensors, a correct adjustment of the spatial features obtained should be achieved (Honkavaara *et al.* 2006). The precision offered by both VHR and Lidar has to be accompanied by a proper accuracy assessment in order to be reliable for forest applications (Hyyppä *et al.* 2000). Otherwise, the integration of these data cannot be properly accomplished, and such synergies will not be highlighted into meaningful indeces, classifications or forest stand parameters. Some authors have encountered difficulties when combining both sources since the accuracy of Lidar is highly superior compared to aerial imagery (Packalen and Maltamo 2007). While Lidar point cloud is orthogonally projected, VHR imagery has to be orthorectified.

In the orthorectifying imagery process, a metrical and homogenous scale document in an orthogonal projection is obtained. VHR aerial photographs acquired on-flight with a matricidal sensor present a strong conical perspective depending on the flight height and the Field of View (FOW). In order to change from conical to orthogonal projection and formulate the topographic correction, internal and external image orientation and a DEM are required (Baltsavias and Käser 1998). Two types of corrections are applied during the orthorectification process of an aerial image: the displacement due to the conic perspective of the original photography and the topography correction. The first component depends on the focal length of the image, radial distance from the projection centre to the object and the height of the vertical element. The topographic correction is made by using the DEM.

Displacement due to the different height of the elements will therefore be affected by the DEM utilized. Fully correction will be achieved if a rigorous model is used, but the object displacement will not be completely corrected if the model is non-rigorous. Most frequently, the bare earth is used as reference surface, by means of a Digital Terrain Model (DTM). As a result, elements above the ground surface are located in a wrong position. In the traditional process of orthorectification of aerial imagery of forest areas, tree presence is consequently not modelled in the DEM. For this reason, trees might show in the orthophoto leaning over canopy gaps or moved from its true location (see Figure 1). In some areas, the usefulness of imagery can be severely affected. Overlaying Lidar and VHR products can be meaningless if, for example, a tree crown is located in the orthophoto where bare soil is shown in a Canopy Height Digital Model (CHDM). In this way, matching different sources of information can be in some cases impossible.

A theoretical orthoimage of ideally straight trees should locate tree tops in the same position where tree bases are; usually, trees appear leaned instead. Lean observed in aerial picture can be caused by many factors:

1. the height of the tree;
2. terrain slope relative to the nadir direction of the picture;
3. natural lean of tree trunks.

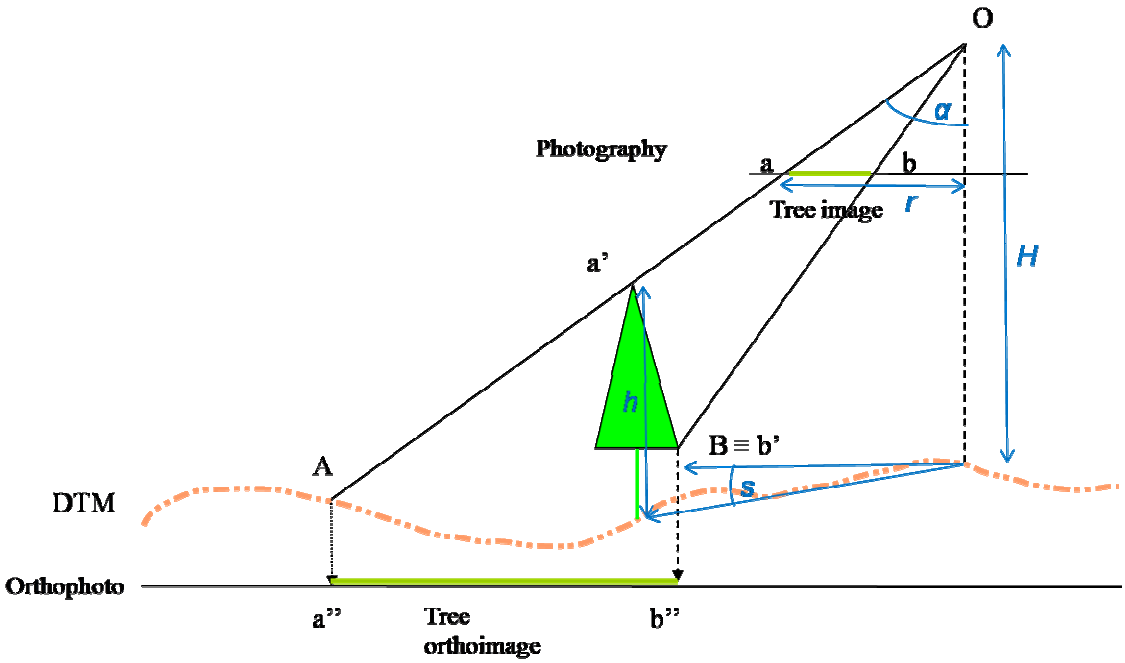

Figure 1: Lean caused by tree height when orthorectifying with a Digital Terrain Model (DTM).

Significant displacement of tree tops might be observed when they are very tall. This lean can be determined as a planimetric distance from where the tree top should be to where it actually appears in meters outwards from the centre of projection. Lean due to tree height can be theoretically calculated as follows (formulae adapted from Molina 2008):

$$dp = h \cdot \mathrm{tg}\ \alpha \qquad (1)$$

This illustrates that the planimetric displacement (dp) of a feature above the DEM used in the orthorectification is a function of the height of the feature from the DEM (h), and the FOV (α). Lean is therefore depending on the height of the elements in the picture, but also on camera and flight parameters: focal length, height of flight and maximum Euclidean distance from nadir direction.

Equation (1) assumes flat terrain, but object lean observed in the image also depends on the slope of the DEM relative to the centre of projection. Objects upslope from the nadir point appear less leaned than calculated in (1), while those downslope appear more leaned (see Figures 2 and 3). This increase or decrease of the observed lean can be added to (1) as a slope component of lean (adapted from Molina 2008):

$$\Delta p = -\, dp \cdot k_s \qquad (2)$$

$$k_s = \mathrm{tg}\ s \,/\, (\mathrm{tg}\ s + \mathrm{tg}\ \alpha) \qquad (3)$$

Hence, displacement is augmented or reduced (Δp) depending on the relative slope (s) between the nadir point and the projection of the element. Δp component will be positive for positions uphill from the centre of projection and negative for elements downhill. Note in Figure 2 and Figure 3 how the real tree top (a') is differently corrected (a'') depending on the topology of the DTM used.

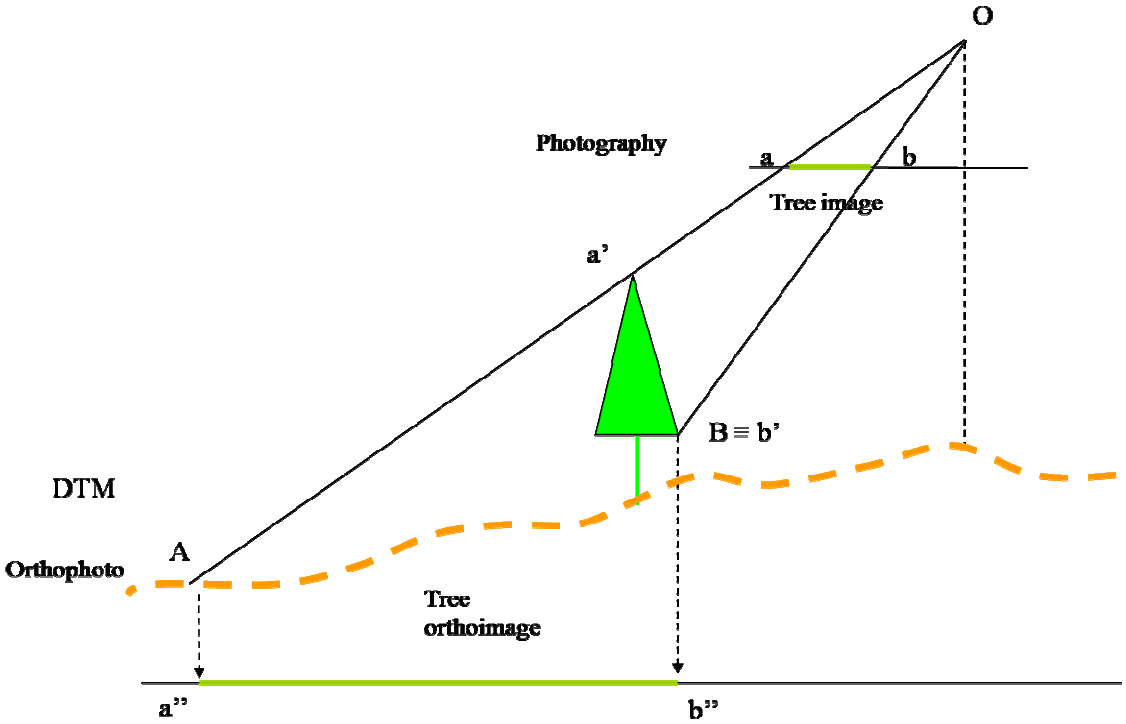

Figure 2: Lean increase due to a downwards slope relative to nadir point.

Another source causing lean in pictures is the real natural lean of tree trunks. This can become significant in a high multi-structured forest. The topography of the study area can make the trunks of trees to be leaned systematically in a certain forest stand. The soil conditions and the relative position of trees themselves are factors affecting random trunk leaning. Random and systematic behaviour of variables describing image lean should therefore be analysed in forest environments.

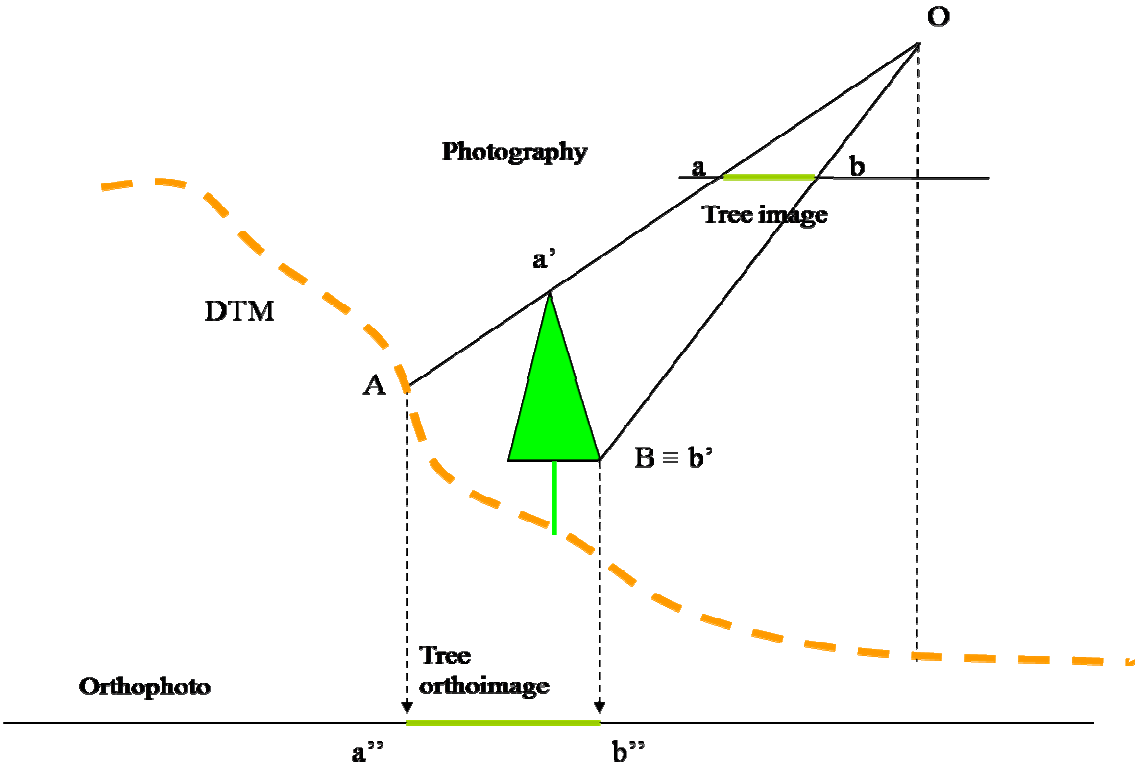

Figure 3: Lean decrease due to an upwards slope relative to nadir point.

Lean problems can be solved by generating a so-called true-ortophoto. Orthorectification of aerial photography over urban areas usually rely on these techniques, since they are highly necessary for avoiding occluded areas when features represented are significantly taller than wider, like buildings are (Schickler and Thorpe, 1998). However, studies using true-orthophoto in forested areas and natural landscapes are scarce (Küchler *et al.* 2004; Waser *et al.* 2008). We hypothesised that employing true-ortophoto can be more useful in order to integrate Lidar and digital camera in forest stands with presence of high trees than results obtained with traditional orthophoto.

Generation of true-orthophoto is based on the use of a Digital Surface Model (DSM) instead of a DTM for correcting the planimetric position of each pixel. When the orthorectifying process is made using a DSM, and every pixel from the resulting orthoimagery has the digital number captured from its real point of view from the sensor. Then, every element is located at its truly orthogonal position (Figure 4). By doing this, whenever a tree crown is repositioned properly, a blind spot occurs. The mosaicking procedure fills these hidden areas from another picture. An analysis of visibility defines the quality of each pixel from the slope relative to the viewing angle, the distance to the centre of projection and the distance to a blind spot. Flight parameters are therefore critical in improving the quality of this process, since better overlapping increases the quality of every pixel and reduces the possibilities of finding areas completely hidden in all pictures (Shiren *et al*. 1989).

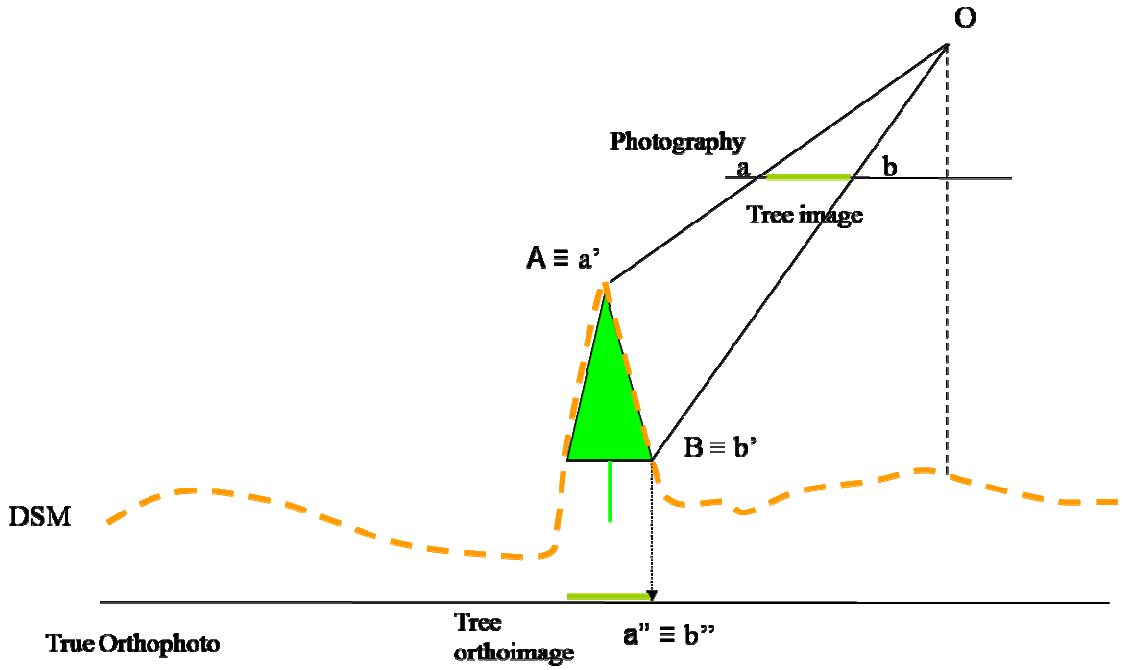

Figure 4: Lean correction by using a Digital Surface Model (DSM) in the orthorectification process.

A comparison of Figure 1 and Figure 4 illustrates how the tree top (a') is located in the orthoimage in a wrong position when using the DTM, but it is coincident with the tree base when using an unrealistically perfect DSM.

2. Material and Methods

2.1 Study area

The study area includes a portion (latitude, 40º53'31" - 41º15'22"N; longitude, 3º59'33" - 4º17'34"W) of the state-owned Scots pine (*Pinus sylvestris* L.) forest of Valsaín, situated in the province of Segovia (Spain). The landscape of the site is characterized by steep slopes, ranging between 10-30%, since it is located in the Central Mountain Range, with elevations between 1265 and 2015 m above European Terrestrial Reference System 1989 (ETRS89). The research has been carried out in a high-relief, dense forest compartment with tall trees, factors which are still challenging for Lidar accuracy (Hyyppä *et al*. 2008), and complicated to orthorectify as well.

2.2 Airborne sensors and dataset

Stereocarto S.L. captured Lidar and imagery simultaneously using the same airborne platform. Both sensors were carried by a CESSNA 404-Titan with double photogrametric window. The flight was performed on September 10, 2006 over a surface area of approximately 800 ha. Flight height was 1500 m above ground.

Lidar scan was made using an ALS50-II sensor from Leica Geosystems, Switzerland. Laser pulse rate was 55 kHz measuring an average of two points per m^2, with footprint diameters of 0.51 m at nadir. A FOV of 25º rendered a 665 m scan width with 40% side lap. Airplane ground speed was 140 knots. A value of intensity was captured for each one of a maximum of four discrete returns per pulse. Recording height accuracy was 0.15 m.

The photogrametric panchromatic, RGB colour, and near infrared images were captured using a DMC camera from Zeiss-Intergraph, Germany. DCM camera has a focal length of 120 mm with a system of frame Charge-Coupled Device (CCD) array sensors. Forward overlap was 60%, while sidelap was 40%. The result was three strips with 55 VHR images of 15 cm ground sample distance and 12 bit of radiometric resolution.

The trajectory and altitude of each sensor was calculated independently using different Global Positioning and Inertial Navigation Systems (GPS/INS). The differential GPS solution was obtained using 3 reference stations: SGVA (designated by Technological Agricultural Institute of Castilla y León Region (ITACYL); latitude: 40º 56' 57,44"N; longitude: 4º 7' 13,21"W), YEBE (designated by Spanish National Geographic Institute (IGN) network; latitude: 40º 31' 29,63"N; longitude: 3º 5' 19,06"W), and MAD2 (designated by NASA worldwide network; latitude: 40º 25' 38,03"N; longitude: 4º 14' 57,08"W). The final positioning trajectory solution was combined from these three reference stations. The spatial reference system was ETRS89. Planimetric coordinates were represented using the Universal Transverse Mercator (UTM) projection, zone 30 north. The altimetric datum was the mean sea level in Alicante, Spain. Elevations were described using orthometric altitudes. The Ibergo95 geoid model was used to transform from elevations over GRS80 ellipsoid to the geoid.

Lidar elevation differences between overlap strips were under sensor tolerance, so that the point cloud was georeferrenced without additional adjustments. The external orientation parameters from the images were obtained using a combined method of direct georeferrence and aerotriangulation using seven control points. Finally, the consistency of both datasets was checked using stereoscopic methods, by viewing the point cloud superimposed over the photogrammetric models of images pairs.

2.3 Lidar products

Prior to obtaining state-of-the-art primary Lidar products such as DTM, DSM and CHDM, the raw cloud point was processed using Terrascan software from Terrasolid, Finland. The first classification step was to remove low and air points. Then, ground points were classified by using the geometric conditions of maximum terrain slope of 75º, iteration angle of 12º and iteration distance of two metres. A filter was applied in search for building points (Axelsson 1999), as some small houses were located in the study area. Finally, unclassified points were considered vegetation class. Quality control of classification was made by an operator using the imagery as a reference data layer.

A one metre regular grid DTM was obtained using a triangulated model from the ground class Lidar points. Intermediate points and last of many returns within 1x1 m cell were removed from vegetation class as a previous step for DSM generation. DSM was then obtained using a triangulated model from ground class points and the remaining vegetation class points. CHDM was finally obtained subtracting DSM minus DTM models.

2.4 Very High Resolution orthoimagery

Traditional orthophoto was obtained from RGB and CIR images by using the Lidar DTM. Co-linearity method was applied for correcting the position. The digital number of each 15 cm pixel was assigned with a bilinear resampling method. Seam line of a final mosaicked product was optimized from the most nadir area from each photograph.

True-orthofoto was obtained as well from RGB and CIR images by using the Lidar DSM. Besides of the topography correction, visibility algorithm was also utilised for detecting occluded areas. Nearest neighbour was used for resampling. Mosaicking was performed for the most nadir areas and for occluded areas too. In the true-orthophoto, no digital number was assigned for pixels without information from any available images, so that they remained as no-data gaps.

2.5 Reference data

A total of six rectangular inventory plots of 40x60 meters were placed in the study area, measuring every tree height with a laser vertex hypsometer. We placed 2-3 landmarks so that every trunk in the plot was able to be aimed at with a Total Station NIKON DTM-332 from Trimble, California. To avoid the obstruction of vegetation, phase differential GPS measurements were taken in October 10, 2007 at nearby positions in absence of canopy cover. Simultaneous GPS observations were also taken at a ground control station in Coberteros (designated by IGN; latitude: 40º42'5,08"N; longitude: 3º57'23,67"W) for differential correction. Static observations were taken with HiperPro receiver from Topcon Positioning Systems Inc., California, and their own software was used for post-processing. The position of tree trunks was finally deducted from a polygonal itinerary between the landmarks and the dGPS occupations. We applied the same transformations described for flight dataset, assuring a proper equivalence. The uncertainty of these measurements was demonstrated to be under a tolerance of ±0.30 m in all cases.

3. Results

A comparison of the Lidar-derived products and the field reference information showed significant correspondences. A pair-wise analysis showed an average difference of 0 ± 0.15 m between the altimetry of the reference dataset and the elevations of the DTM product (see Figure 5); the accuracy of georeferring processes and the precision of the sensor were therefore confirmed. When validating for the inventory, CHDM tended to underestimate tree height, since the presence of outliers showed few planimetric mismatches in a discrete tree-by-tree comparison without any correlation algorithm for spatial matching. This is explained because the real orthogonal projection on the ground of some tree tops is not coincident with the tree base, due to the presence of naturally leaned trunks in the study area. This leads to a high presence of random noise in every planimetric tree-by-tree analysis. Nevertheless, no systematic lean tendencies were found in the study area.

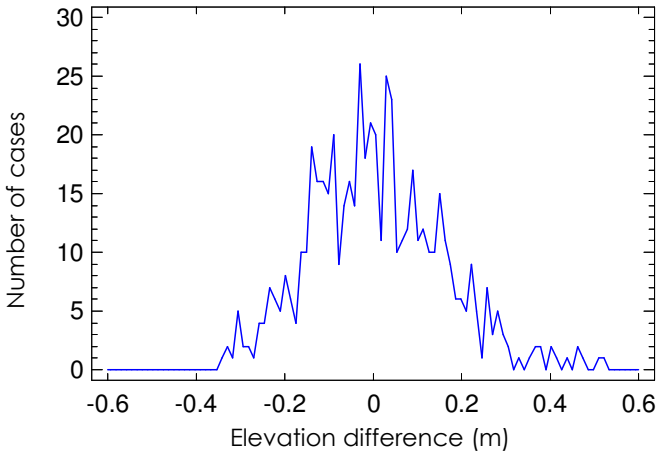

Figure 4: Histogram of elevation differences between the reference ground truth and the Lidar-derived Digital Terrain Model (DTM).

Contrary to the other two information datasets, orthorectified aerial imagery showed important displacements of planimetric information. This led to significant mismatching of Lidar products with imagery products, *i.e.* indices, classifications and photo-interpreted features. This was of critical importance, since integration of sensors was therefore unsuccessful in many cases. In order to distinguish displacements caused by random tree trunk lean from picture lean, the spatial distribution of planimetric errors was compared to the theoretical lean of trees calculated from (1) and (2). For this certain focal length, since the FOV (α) in the position of each tree top is depending on the Euclidean distance to the nadir point of the projection in the image space (r) and the difference between the flight (H) and tree (h) heights, equation (1) can be reformulated as:

$$dp = h \cdot r / (H - h) \qquad (4)$$

The theoretical spatial distribution of lean errors was calculated for every position in the study area by using the calculated CHDM elevation as tree height in the formula (4), and the DTM positions to calculate the relative slope of each pixel to its centre of projection in (2) and (3) (see Figure 5). Real displacements were measured as the planimetric Euclidean distance between the tree base reference data and the tree top interpreted at the orthoimage. Observed lean showed a significant correlation with theoretical lean, presenting the same spatial distribution pattern. This demonstrated that the mismatching was provoked by the perspective itself, and not just randomly distributed natural trunk lean.

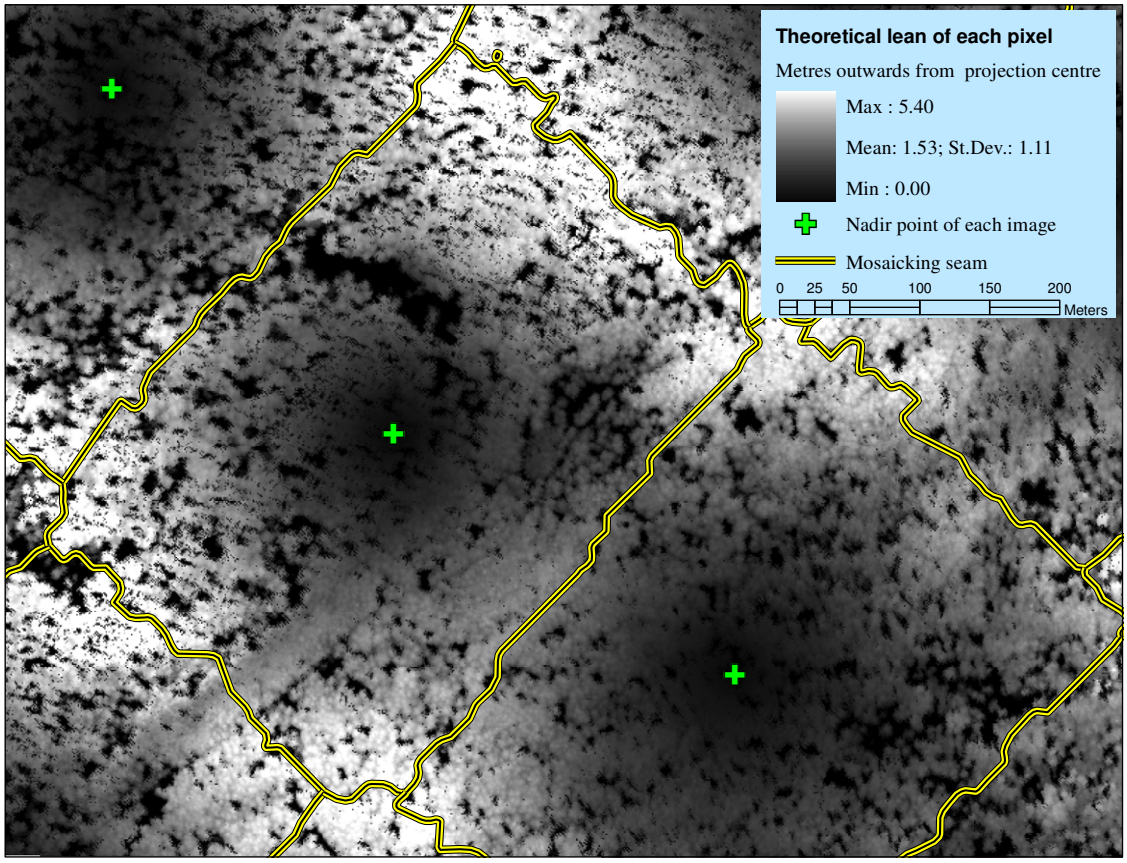

Figure 5: Raster model showing the spatial pattern distribution of lean suffered by each pixel.

Tree tops observed from true-orthophotography were also compared with the reference position of their correspondent base. Planimetric mismatching was significantly reduced compared to traditional ortophoto. True-orthoimagery was verified as a reliable methodology for improving geometrical accuracy of aerial information, as shown in Figure 6. Errors were distributed randomly and showed no spatial pattern, so that they can be assumed to be dependent on other factors than the Euclidean distance to the nadir point of the picture. However, individual tree shapes were found distorted in many cases, so that true-imagery is less practicable for photo-interpretation purposes than traditional DTM-derived orthophoto. Isolated tree crowns showed more deformities than stands presenting continuous canopies; these results are coherent with those obtained by other authors (Leckie *et al.* 2003).

4. Discussion

Simultaneous acquisition of Lidar in a photogrametric flight notably increases the automation of the procedures and reduces processing time and costs for orthoimagery production. Lidar obtains mass points automatically, therefore reducing the need for quality control and minimising error occurrence. Thus, traditional photogrametric correlation was still challenging in densely forested canopies, so Lidar introduced an exceptional advantage concerning DEM calculation from photogrametric flight. VHR imagery needs to rely on precise data that only Lidar can nowadays offer.

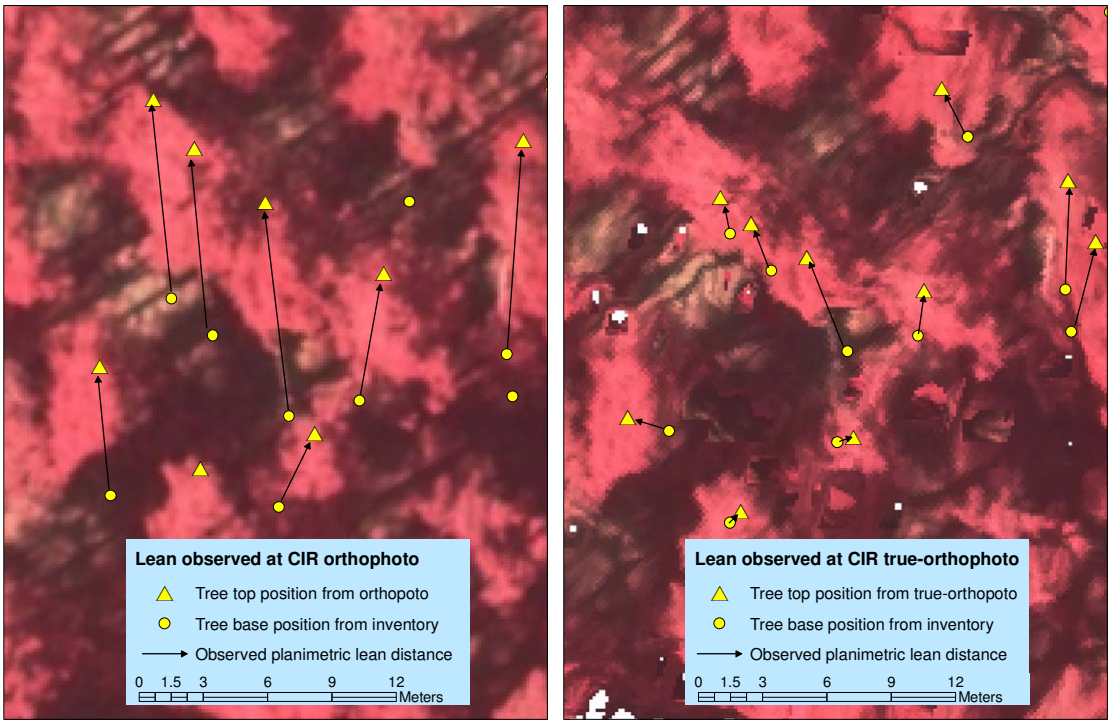

Figure 6: Comparison of mismatching between planimetric positions of tree base measured in the field and tree top position interpreted from false colour infrared orthophoto (left) and true-orthophoto (right).

In order to integrate information simultaneously obtained from different sensors, a proper geometric correspondence between them has to be accomplished. Terrain slope and tree height were found as factors of relevant importance in increasing the difficulties of achieving the orthogonal location of features in aerial imagery. Lean of tree tops in orthoimagery was demonstrated to be caused by the presence of tall trees and steep terrain.

True-orthorectification of aerial imagery has improved significantly the planimetric adjustment of tree tops. Nevertheless, radiometric properties have suffered numerous deficiencies. The consistency and usefulness of the radiometric information has still to be tested in true-orthophotos. Thus, DSM-derived orthophoto contained numerous artefacts and no-data gaps, due to the visibility analysis' process. Photo-interpretation of features is more difficult than those in traditional orthophoto. Distortion of tree crown may reduce the possibilities of any analysis of texture or crown shape.

Alternative possibilities for solving lean problems in future flights over high canopies in mountainous areas concern changes in:

1. the digital camera;
2. flight parameters;
3. alternatives for orthophoto calculation; like those discussed in this article.

The displacement of the vertical objects in the photographic images can be reduced using larger focal length, or using linear array sensors with pushbroom technology instead of CCD array ones, where vertical displacement is bidirectional instead of radial. Linear array would accomplish lean errors to be distributed transversally to the flight line direction. Flight parameters should be modified by increasing the sidelap in order to optimise mosaicking procedures. Changes in flight height are not considered since spatial resolution would be reduced.

Acknowledgements

Authors want to thank the Spanish *Ministerio de Industria, Turismo y Comercio* (MITYC) who funded this study within the research project "LINHE: Desarrollo de nuevos protocolos de integración de sensores LiDAR, cámara digital, IR cercano e hiperespectral" (project: FIT-330221-2006-10). Partner institutions of LINHE project are: Stereocarto S.L.; GMV Aerospace and Defence S.A.; TRAGSA; University of Córdoba (UCO); and Technical University of Madrid (UPM).

References

Axelsson, P. 1999. Processing of laser scanner data – algorithms and applications. *ISPRS Journal of Photogrammetry and Remote Sensing*, 54, 138-147.

Baltsavias, E. and Käser, Ch. 1998. DTM and orthoimage generation — a thorough analysis and comparison of four digital photogrammetric systems. Int. Arch. Photogramm. Remote Sens. 32 (4), 42–51.

Leckie, D.G., Gougeon, F.A., Walsworth, N. and Paradine, D. 2003 Stand delineation and composition estimation using semi-automated individual tree crown analysis. *Remote Sensing of Environment*, 85 (3), 355-369.

Leckie, D.G., Gougeon, F.A., Tinis, S., Nelson, T., Burnett, C.N. and Paradine, D. 2005 Automated tree recognition in old growth conifer stands with high resolution digital imagery. *Remote Sensing of Environment*, 94 (3), 311-326.

Honkavaara, E., Ahokas, E., Hyyppä, J., Jaakkola, J., Kaartinen, H., Kuittinen, R., Markelin, L. and Nurminen, K. 2006. Geometric test field calibration of digital photogrammetric sensors. *ISPRS Journal of Photogrammetry and Remote Sensing*, 60 (6), 387-399.

Hyyppä, J., Hyyppä, H., Inkinen, M., Engdahl, M., Linko, S. and Yi-Hong, Z. 2000. Accuracy comparison of various remote sensing data sources in the retrieval of forest stand attributes. *Forest Ecology and Management*, 128, 109–120.

Hyyppä, J., Hyyppä, H., Leckie, D., Gougeon, F., Yu, X. and Maltamo, M., 2008. Review of methods of small-footprint airborne laser scanning for extrcting forest inventory data in boreal forests. *International Journal of Remote Sensing*, 29, 1339-1366.

Küchler, M., Ecker, K., Feldmeyer-Christe, E., Graf, U., Küchler, H. and Waser, L.T. 2004. Combining remotely sensed spectral data and digital surface models for fine-scale modelling of mire ecosystems. *Community Ecology*, 5(1), 55–68.

Lefsky, M.A., Cohen, W.C., Acker, S.A., Parker, G.G., Spies T.A. and Harding, D. 1999. Lidar remote sensing of the canopy structure and biophysical properties of douglas-fir western hemlock forests. *Remote Sensing of Environment*. 70, 339–361.

Molina, S. 2008. Departamento de fotogrametría de TRAGSATEC. Jornadas Técnicas del Plan Nacional de Ortofotografía.

Packalen, P. and Maltamo, M. 2007. The k-MSN method for the prediction of species-specific stand attributes using airborne laser scanning and aerial photographs, *Remote Sensing of Environment*, 109 (3), 328-341.

Schickler, W. and Thorpe, A 1998. Operational procedure for automatic true orthophoto generation. *Int. Arch. Photogramm. Remote Sens*. 32 (4), 527–532.

Shiren, Y., Li, L. and Peng, G., 1989. Two-dimensional seam-point searching in digital image mosaicking. *Photogramm. Eng. Remote Sens*. 55 (1), 49–53.

St-Onge, B.A. and Cavayas, F. 1997. Automated forest structure mapping from high resolution imagery based on directional semivariogram estimates. *Remote Sensing of Environment*, 61 (1), 82-95.

St-Onge, A. and Achaichia, N. 2001. Measuring forest canopy height using a combination of LiDAR and aerial photography data. *International Archives of Photogrammetry and Remote Sensing*, XXXIV-3/W4, 131−137.

Suárez, J., Ontiveros, C., Smith, S. and Snape S. 2005. Use of airborne LiDAR and aerial photography in the estimation of individual tree heights in forestry. *Computers & Geosciences*, 31, 253–262.

Waser, L.T., Baltsavias, E., Eckera,K., Eisenbeiss, H., Feldmeyer-Christe, E.H., Ginzler, C., Küchler, M. and Zhang L. 2008. Assessing changes of forest area and shrub encroachment in a mire ecosystem using digital surface models and CIR aerial images. *Remote Sensing of Environment*, 112, 1956–1968.

Zhang, L. and Gruen, A. 2004. Automatic DSM Generation from linear array imagery data. *International archives of photogrammetry, Remote Sensing and Spatial Information Sciences*, 35 (B3), 128−133.